

This is the accepted version of the following article:

Trummer, G., Buckley-Johnstone, L. E., Voltr, P., Meierhofer, A., Lewis, R., & Six, K. (2017). Wheel-rail creep force model for predicting water induced low adhesion phenomena. *Tribology International*, 109, 409-415. doi:10.1016/j.triboint.2016.12.056

This postprint version is available from <http://hdl.handle.net/10195/67456>

Publisher's version is available from <http://www.sciencedirect.com/science/article/pii/S0301679X16305412>



This postprint version is licenced under a [Creative Commons Attribution-NonCommercial-NoDerivatives 4.0 International](https://creativecommons.org/licenses/by-nc-nd/4.0/).

Wheel-rail creep force model for predicting water induced low adhesion phenomena

G. Trummer^a, L.E. Buckley-Johnstone^b, P. Voltr^c, A. Meierhofer^a, R. Lewis^b, K. Six^a

^a Virtual Vehicle Research Center, Graz, Austria

^b Department of Mechanical Engineering, The University of Sheffield, Sheffield, UK

^c Jan Perner Transport Faculty, University of Pardubice, Pardubice, Czechia

Abstract

A computationally efficient engineering model to predict adhesion in rolling contact in the presence of water is presented which may be implemented in multibody dynamics software or in braking models to study train performance and braking strategies. This model has been developed in a project funded by the Rail Safety and Standards Board (RSSB) and Network Rail. It is referred to as the water-induced low adhesion creep force (WILAC) model. The model covers a wide range of conditions from dry over damp to wet. Special emphasis is put on little amounts of water which can cause low adhesion without any oil or grease. Such conditions may be encountered in humid weather or at the onset of rain. The model is parameterised based on experimental results from a tram wheel test rig. Adhesion values as low as 0.06 are observed at high creep with only wear debris and little water present in the contact. The model results also agree with experimental data from locomotive tests in dry and wet conditions.

Nomenclature

A	Ratio of friction coefficient at infinite slip velocity to μ_0 in the Polach model
a	Semi-major axis length of Hertzian contact ellipse
B	Decay constant in the friction law of the Polach model
b	Semi-minor axis length of Hertzian contact ellipse
c_x	Longitudinal creep
c_y	Lateral creep
c_z	Spin creep
e	Transition functions in the WILAC model
f	Weights for blending of conditions in the WILAC model
k_A	Stiffness reduction factor in the area of adhesion in the Polach model
k_S	Stiffness reduction factor in the area of slip in the Polach model
m	Reference water flow rate of transition between conditions in the WILAC model
μ_0	Maximum friction coefficient in the Polach model
Q	Normal force
s	Width of transition between conditions in the WILAC model
T	Creep force
T_x	Longitudinal creep force
T_y	Lateral creep force
T/Q	Adhesion value
v	Rolling speed
w	Water flow rate

1. Introduction

For braking of railway vehicles a minimum adhesion of approximately 0.15 is usually required between wheels and rails for safe operation [1]. Adhesion values $T/Q < 0.15$ may be referred to as “low adhesion” [2].

In Great Britain during the autumn period (from October to November) numerous incidents, such as “station overruns” and signals passed at danger (SPADs) occur every year which are related to low adhesion conditions [3]. For about half of the incidents an autumn leaf contamination has been reported [3] which is known to cause low adhesion [4]; [5]; [6]; [7]; [8]. A proportion of the other half were related to small amounts of water on the rail head caused by prevailing environmental conditions. Detailed analysis shows a peak in incidents, for example, around dew point conditions in the morning and evening [9]. There is also experimental evidence that low amounts of water in combination with iron oxides on the surface reduce adhesion in rolling contacts without the presence of other contaminants [10].

The objective of this work was to develop a computationally efficient creep force model which is able to predict adhesion depending on the “wetness” of the surface. The focus is on low amounts of water causing low adhesion conditions in the absence of oil or grease. Model development is accompanied by experiments on a tram wheel test rig which provided data for the model parameterisation. The model may be used in multibody dynamics (MBD) simulations to study the effect of low adhesion on train performance, or it may be implemented in braking models to study possible braking strategies.

2. Influence of water on adhesion

Two mechanisms govern the adhesion in rolling contact in the presence of interfacial fluids: Boundary lubrication and hydrodynamic lubrication. The transition region where both mechanisms govern adhesion is referred to as mixed lubrication. Which mechanism dominates depends on the relative velocity between the surfaces, the fluid viscosity and the normal force [11]. In addition the size and the shape of the contact patch and the surface roughness play a role [12].

Creep curves (adhesion as a function of creep) in dry conditions differ from creep curves in wet conditions with respect to the adhesion level, the shape of the curve and the initial slope [13]. Wetting the surface with water reduces the adhesion level, shifts the adhesion maximum to higher creep values and reduces the decrease of adhesion with increasing creep [13].

Measurements with various locomotives show that the maximum adhesion value is around 0.35 in dry conditions at low speeds [13]. In test rig experiments maximum adhesion values between 0.5 and 0.6 have been observed for axle loads of 44 kN and 67 kN [14]. Locomotive tests with an axle load of 220 kN showed maximum adhesion values between 0.3 and 0.4 for rolling speeds from 5 m/s to 20 m/s [15].

In the presence of water maximum adhesion values drop with respect to dry conditions. A typical value of 0.25 has been found in locomotive tests in wet conditions at low speeds [13]. Test rig results showed maximum adhesion values ranging from 0.10 to 0.16 at a speed of 100 km/h for axle loads of 44 kN and 67 kN [14]. In locomotive tests maximum adhesion values of 0.25 have been observed at axle loads of 220 kN at a speed of 10 m/s with artificially watered rails [15]. Small-scale laboratory experiments on a ball-on-disc machine showed a typical maximum adhesion value of 0.15–0.20 for a roughness of $R = 0.15 \mu\text{m}$ at rolling speeds of 1.5 m/s when submerged in water [16].

Chen et al. investigated the influence of rolling speed, surface roughness, maximum contact pressure, and water temperature on the maximum adhesion in Twin Disc experiments in wet conditions. The results

show that high rolling speeds, smooth surfaces and low water temperatures can lower the adhesion to values of 0.02 [17].

Beagley and Pritchard [10] investigated the change of adhesion over time in an Amsler experiment, where two steel discs roll on each other with a fixed (longitudinal) creep of 0.033 at a circumferential velocity of about 0.3 m/s (see Fig. 1). When water is applied to the contact the adhesion drops from around 0.6 to around 0.3. When the wet surfaces are allowed to dry a viscous paste of wear debris and water forms on the surface which reduces the adhesion to a minimum value of 0.2 before the dry adhesion value is observed again. If the generated wear debris in the rolling contact is continuously removed from the surface by a wire brush, no adhesion minimum is observed [10].

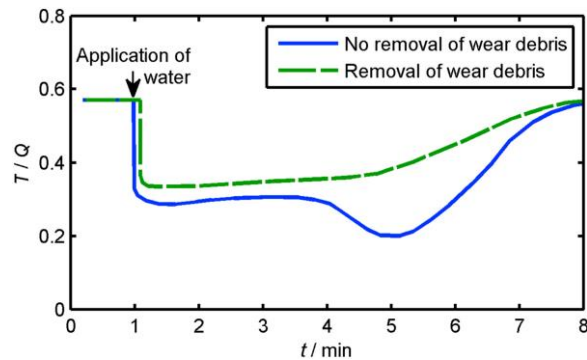


Fig. 1. Schematic change of adhesion T/Q in an Amsler experiment when the surface dries up after an initial application of water; Solid line: Adhesion minimum without continuous removal of wear debris; Dashed line: Continuous removal of wear debris by wire-brushing the surface; data reproduced from [10].

These experiments demonstrate that wear debris in combination with little amounts of water reduce adhesion to values well below the adhesion value when large amounts of water are present on the surface [10]. However, the observed minimum adhesion values cannot be considered “low adhesion”.

3. Existing creep force models taking the effect of water into account

Several creep force models already exist which take the influence of water on adhesion into account in various ways.

Kalker's half-space model CONTACT [18] considers boundary lubrication only. The influence of water on adhesion is usually included by adjusting the constant values of the static and dynamic coefficient of friction. Recent extensions of CONTACT [19] include the implementation of a falling friction law and the implementation of an elastic interfacial layer.

Likewise, in the simplified theory of rolling contact, which is implemented in the algorithm FASTSIM [20], the influence of water can be considered by adjusting the constant coefficient of friction in terms of boundary lubrication. Spiryagin [21] extended the FASTSIM algorithm by a variable contact flexibility and a slip dependent friction law (variable friction coefficient) to allow a better reproduction of measured creep curves.

The Polach model [13]; [22] is a computationally fast alternative to the FASTSIM algorithm, built on the theory of boundary lubrication as well. The model can be tuned to experimental results under wet conditions by adjusting the initial slope of the adhesion curve and the decrease of adhesion with increasing slip velocity (variable friction coefficient). The amount of water is not explicitly taken into account.

Beagley [23] estimated adhesion in the wheel/rail contact based on hydrodynamic lubrication theory assuming full sliding. Key input parameters are the viscosity of the iron oxide/water mixture and the film thickness on the rail. This model is not a full creep force model, so that adhesion at low creep cannot be calculated.

The Chen model [24]; [25] uses both boundary lubrication theory and hydrodynamic lubrication theory. Adhesion under wet conditions for rough surfaces is predicted by distributing the load between contact asperities experiencing boundary lubrication (with constant friction coefficient) and the hydrodynamic water film based on statistical methods. Key input parameters are the surface roughness and the fluid viscosity.

The Popovici model [26] uses boundary lubrication theory (with a constant friction coefficient) for the contact between surface asperities and hydrodynamic lubrication theory to describe the behaviour of the fluid layer. The model takes rough surfaces, frictional heating in the elasto-hydrodynamic component and starved contact conditions (limited supply of liquid to the contact) into account.

The Tomberger model [12] combines the FASTSIM algorithm with an interfacial fluid model, a temperature model and a micro-contact model. Fluid related input parameters are the viscosity and the amount of liquid on the rail surface. The (variable) friction coefficient in the micro-contact model is a function of the local contact conditions.

The Zhu model [28] comprises of a normal contact model, an interfacial fluid model based on hydrodynamic lubrication theory and a tangential contact model. The model has been used with measured 3D surfaces to estimate adhesion.

The Extended Creep Force (ECF) model [15]; [27] extends the Tomberger model by a temperature- and normal stress-dependent elasto-plastic third-body layer model. Adhesion is governed by the solid interfacial layer whose properties are changed by interfacial fluids.

For the objective of this work computational efficiency, a fully published model structure and the ability of the model to describe complex adhesion characteristics are crucial points. With respect to applicability in the practice of railway operation a simple approximate engineering model with a minimum of (well-known) input parameters is preferred over a detailed and sophisticated model. In railway operation little amounts of wear debris in combination with water are expected at the rail surface so that mainly boundary lubrication with some influence of hydrodynamic lubrication (creating a mixed lubrication condition) may be assumed.

Considering all these points the Polach model (based on boundary lubrication theory) seems to suit these needs best, thus the Polach model has been chosen as the basis for the development of the WILAC model, which is described in Section 5.

4. Tram wheel test rig experiments

Experiments at a tram wheel test rig at the University of Pardubice have been performed to clarify the effect of water on adhesion in rolling contacts in a large creep range.

The tram wheel test rig comprises of a full-size tram wheel (diameter 0.696 m, material equivalent to material B6 in standard UIC 810-1) and a rail roller (diameter 0.905 m, material equivalent to material BV 2 in standard UIC 810-1). The effective radius in lateral direction of the contact was estimated to be 0.660 m based on imprints of the contact patch on carbon paper. The normal load is applied to the wheel by an air spring. The rail roller with the torque transducer is kept at constant rotational speed during the experiment.

To record adhesion as a function of creep the circumferential velocities of the wheel and the rail roller are brought to the desired value. Then a slowly increasing torque is applied to the wheel over a period of typically 15–20 s, while the rail roller is kept at the pre-set constant circumferential velocity. When large sliding of the wheel is detected, the torque applied to the wheel is reduced to zero and free rolling resumes. A typical sliding event lasts approximately 5 s. During an experiment the torque is increased and decreased multiple times. From the measured torque at the rail roller and the rotational speed of the wheel and the rail roller (measured by rotary encoders) adhesion curves can be deduced. Usually traction is applied to the wheel to prevent damage to the surface caused by a blocking wheel. Further details about the test rig can be found in [29].

The sensors for measuring the normal force and the torque at the test rig have been calibrated by static tests prior to the experiments. The measurement uncertainty of the adhesion value may be estimated as two times the standard deviation of repeated torque calibration data at 4.2 kN normal force. Based on the torque calibration data the uncertainty of the adhesion value is approximately 0.02.

Adhesion curves have been recorded for a normal contact force of 4.2 kN at a rolling speed of 5 m/s. Temperature and relative humidity were uncontrolled at the test rig. During the experiments the temperature ranged from 20 °C to 25 °C, and the relative humidity was between 54%RH and 70%RH. To realize low amounts of water in the wheel/rail contact, water has been applied drop-wise to the rotating rail roller at a constant rate by a gravity fed application system (see Fig. 2). This application method has been found to work reliably for rolling speeds up to 7 m/s.

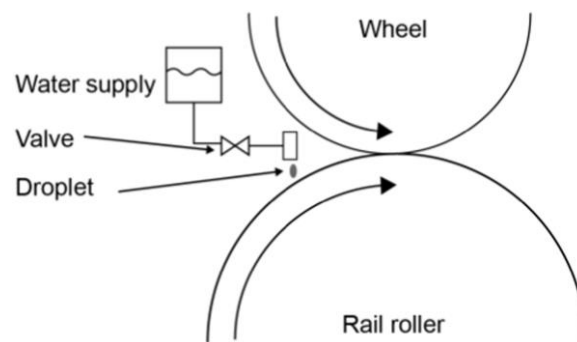


Fig. 2. Drop-wise application of low amounts of water by a gravity fed water application system at the tram wheel test rig.

Water drop rate was controlled by a valve. The end of the pipe where the droplets formed was brought as close as possible to the contact. With this setup average water flow rates of 25 $\mu\text{l/s}$, 35 $\mu\text{l/s}$, and 60 $\mu\text{l/s}$ were realized. The measured average water volume of one drop is about 60 μl . The water rate of 350 $\mu\text{l/s}$ was realized by using a micro-pump.

Multiple adhesion curves have been recorded in dry condition and for different water flow rates. The results are shown in Fig. 3.

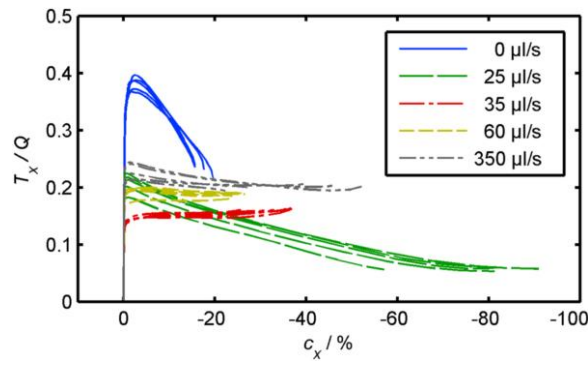


Fig. 3. Measured adhesion T_x/Q as a function of longitudinal creep c_x in the tram wheel test rig experiments as a function of the water flow rate at 4.2 kN normal force and 5 m/s rolling speed.

The experimental data show two types of adhesion characteristics: The “dry” type (observed at water flow rates 0 $\mu\text{l/s}$ and 25 $\mu\text{l/s}$) shows a peak adhesion at low creep in combination with a steep decrease of adhesion with increasing creep.

Typical for the “wet” type (observed at water flow rates 35 $\mu\text{l/s}$, 60 $\mu\text{l/s}$ and 350 $\mu\text{l/s}$) is an almost constant adhesion value with increasing creep.

The adhesion curve at a water flow rate of 25 $\mu\text{l/s}$ is particularly interesting, because the peak adhesion value at low creep is comparable to the peak adhesion values observed at higher water flow rates. But in contrast to other wet curves, a strong reduction of the adhesion value with increasing creep is observed in this case. Adhesion values of 0.06 have been measured repeatedly in the creep range from -60% to -90% .

5. WILAC model

The WILAC model (acronym for Water-Induced Low Adhesion Creep Force Model) describes the wheel/rail adhesion in dry, moist and wet conditions with special emphasis on moist conditions. In the model the wetness of the contact surface is quantified in terms of a water flow rate w to the surface.

The structure of the WILAC model is shown in Fig. 4. It consists of linear regression models, a Polach creep force model and a function for blending in between conditions. These parts of the WILAC model are described in the following sections.

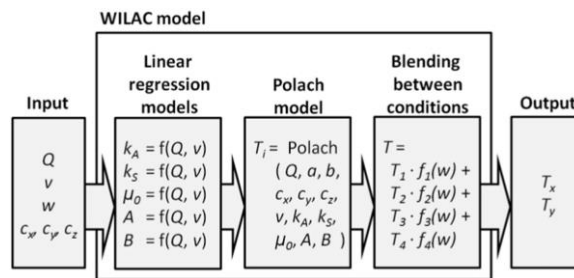


Fig. 4. General structure of the WILAC model for calculating creep forces in dry, moist and wet conditions.

5.1. Creep force calculation

The WILAC model for estimating the wheel/rail adhesion is built around the Polach model [22]. The Polach model is a state-of-the-art creep force model which is extensively used in multibody simulations of railway vehicles. It calculates the longitudinal and lateral creep forces T_x and T_y as a function of the contact normal force Q , of the semi-major axis length a and the semi-minor axis length b of the Hertzian contact

ellipse, and the relative motion between the surfaces in terms of longitudinal creep c_x , lateral creep c_y , and spin creep c_z .

The original model has been extended to consider the decrease in adhesion with increasing relative velocity between the contact surfaces and to consider the experimentally observed reduction of the initial gradient of the creep curve [13]. These features are described by five Polach model parameters: k_A and k_S , which are related to the gradient of the adhesion curve at low creep; and A , B , and μ_0 which are related to the decrease of adhesion at high creep values.

5.2. Linear regression models

Linear regression models have been implemented for the (internal) calculation of the Polach parameters in the WILAC model because the observed change of the adhesion characteristic as a function of vehicle speed and normal force does not agree well with available experimental data from locomotive tests [15] when fixed values are used for the Polach parameters in the calculation.

Experimental data from the tram wheel test rig were not available for the whole range of operating conditions with respect to normal force and rolling speed for the WILAC model development. Thus, extrapolation of data to a wider range of normal forces and rolling speeds was necessary, which was done with the Extended Creep Force (ECF) model [15]; [27].

The ECF model explicitly considers third-body layers and the effects of plastic deformation, material hardening, and temperature-related softening of this layer on the adhesion level. Therefore the model behaviour of the ECF model differs from that of the Polach model with respect to normal force and rolling speed.

Adhesion curves calculated with the ECF model can be reproduced with a Polach model by individually adjusting the Polach parameters for each adhesion curve. If the ECF model behaviour needs to be reproduced over a whole range of normal forces and vehicle speeds, the Polach parameters of the Polach model need to be adjusted for each combination of normal force Q and rolling speed v . The necessary adjustment of the Polach parameters is done by five linear regression models in the WILAC model which calculate the (internal) parameters k_A , k_S , A , B , and μ_0 as a function of the normal force Q and the vehicle speed v .

For example, a multiple linear regression model relating parameter k_A to the normalized normal contact force Q' and to the normalized rolling speed v' can be chosen as:

$$k_A = a_0 + a_1 Q' + a_2 v' + a_3 Q'^{-1} + a_4 v'^{-1} + a_5 e^{Q'} + a_6 e^{v'} + \dots + e$$

Therein, k_A is the dependent variable. Q' and v' are the independent variables, which are normalized to their maximum values in the investigated parameter range. a_i are the regression coefficients and e is an error term. The terms Q' , Q'^{-1} , $e^{Q'}$, v' , v'^{-1} , and $e^{v'}$ up to order 3 including mixed terms are used as independent variables in building the regression model. The regression coefficients a_i are determined by the method of least squares based on i observations of the dependent variable k_A . Only those independent variables, which improve the R^2 -value by at least 10^{-4} are included in the regression model.

For each of the Polach parameters k_A , k_S , μ_0 , A , and B separate multiple linear regression models are set up. The R^2 -values of these regression models are typically equal or better than 0.996.

5.3. Blending between conditions

The WILAC model has been parameterised based on four representative conditions (Dry, Damp2, Damp1, Wet) associated with different degrees of wetness of the surface. For each condition an independent set of

linear regression models for estimating the (internal) Polach parameters has been determined based on the experimental data and the data extrapolation as described in Section 5.2.

Because the experimental data have been recorded at fixed water flow rates an interpolation method is needed to be able to change the water flow rate continuously in the WILAC model. Thus, the actual longitudinal adhesion T_x/Q (and the lateral adhesion T_y/Q) as a function of the water flow rate w is determined by interpolating between the four representative conditions according to the following weighted sum:

$$\frac{T_{i=x,y}}{Q} = \frac{1}{Q} (f_{Dry} \cdot T_{i,Dry} + f_{Damp2} \cdot T_{i,Damp2} + f_{Damp1} \cdot T_{i,Damp1} + f_{Wet} \cdot T_{i,Wet})$$

The weights f_i as a continuous function of the water flow rate w are shown in Fig. 5.

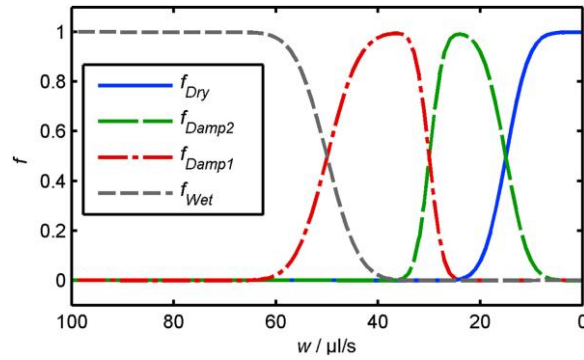


Fig. 5. Weights f_i which are used to calculate the adhesion T_i/Q , as a function of water flow rate w .

The weights f_i are derived from three functions e_1 to e_3 defined as:

$$f_{Dry} = 1 - e_1$$

$$f_{Damp2} = e_1 - e_2$$

$$f_{Damp1} = e_2 - e_3$$

$$f_{Wet} = e_3$$

Functions e_1 to e_3 are related to the transitions between the conditions. They are chosen as:

$$e_i = \frac{1}{2} \left(\operatorname{erf} \left(\frac{w - m_i}{s_i} \right) + 1 \right)$$

m defines the position of the transition with respect to the water flow rate w , while s specifies the width of the transition. Functions e_1 to e_3 are shown in Fig. 6 and the associated parameters m and s are given in Table 1.

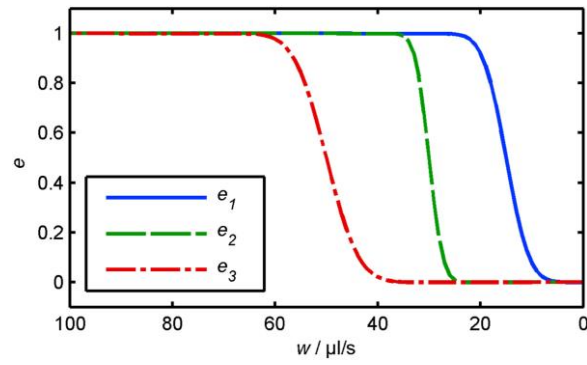


Fig. 6. Transition functions e_1 to e_3 used to derive the weights f_i .

Table 1. Parameters m and s for transition functions e_1 to e_3 used to describe the transitions between different surface conditions.

Function	Transition	$m/(\mu\text{l/s})$	$s/(\mu\text{l/s})$
e_1	Damp2 – Dry	15	5
e_2	Damp1 – Damp2	30	3
e_3	Wet – Damp1	50	7

The mathematical structure of e_1 , e_2 and e_3 does not follow from the experimental results but is motivated to ensure smooth transitions between the adhesion conditions (Dry, Damp2, Damp1, Wet) and to allow a convenient adjustment of the individual transitions with respect to position and width according to experimental data.

5.4. Model parameterisation and validation

Four representative experimental datasets from the tram wheel test rig experiments with respect to the water flow rate w have been used for the WILAC model parameterisation (see Section 4). These were the “Dry” data, the damp datasets recorded at water flow rates of 25 $\mu\text{l/s}$ and 35 $\mu\text{l/s}$ (“Damp2”, “Damp1”) and the “Wet” dataset recorded at a water flow rate of 350 $\mu\text{l/s}$. Each of these experimental data (at fixed water flow rate w) were recorded at a normal force of 4.2 kN and a rolling speed of 5 m/s. These data were extrapolated to a wider range of operating conditions with the ECF model [15]; [27], which was parameterised based on locomotive test data previously. The experimental data and the extrapolated data then served as the basis for the determination of the linear regression models for the (internal) calculation of the Polach parameters in the WILAC model (see Section 5.2).

Fig. 7 shows the WILAC model results after the final model parameterisation (thick lines) together with the underlying experimental data used for model parameterisation (thin lines).

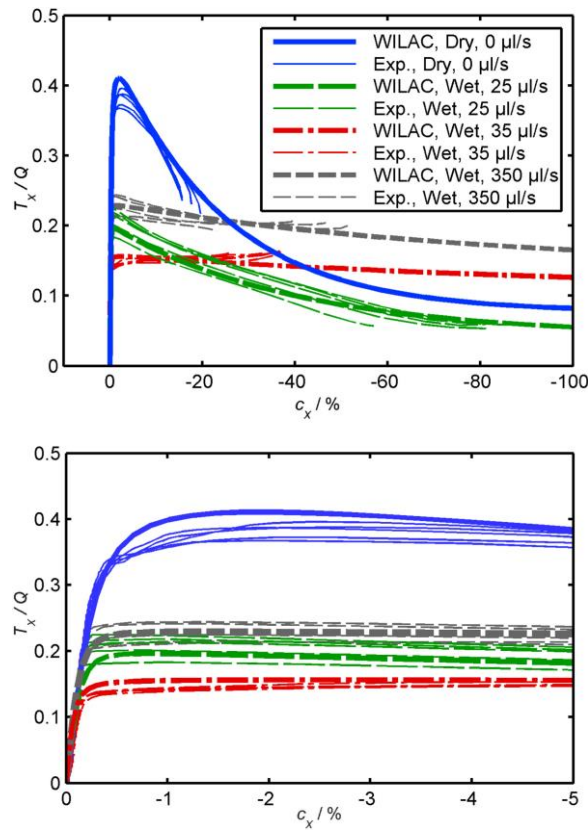


Fig. 7. Comparison of adhesion T_x/Q as a function of longitudinal creep c_x for different water flow rates at 4.2 kN normal force and 5 m/s rolling speed: Data from tram wheel test rig experiments (thin lines), WILAC model results after parameterisation with tram wheel test rig data (thick lines); Top: Full dataset, Bottom: Detail of low creep range.

Fig. 8 shows the change of the adhesion for different fixed longitudinal creep values c_x as a function of the water flow rate w calculated with the WILAC model. Depending on the longitudinal creep adhesion minima are obtained for water flow rates in the range from 20 $\mu\text{l/s}$ to 40 $\mu\text{l/s}$. The shape of the curve at $c_x = -3\%$ is very similar to the adhesion curve reported by Beagley and Pritchard without removal of wear debris from the surface (see Fig. 1).

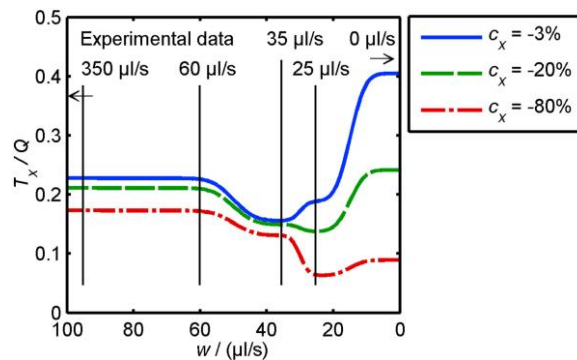


Fig. 8. Change of adhesion T_x/Q as a function of water flow rate w for different fixed values of longitudinal creep c_x in the WILAC model. Water flow rates w where experimental data have been recorded are marked by vertical lines.

Fig. 9 compares WILAC model results to experimental adhesion data from full-scale locomotive tests in dry condition for different rolling speeds. Results have also been compared in wet condition (see Fig. 10), where the track was artificially watered (flooded conditions). These locomotive tests have been recorded at a normal contact force of 110 kN, which is significantly higher than the normal contact force used in the experiments at the tram wheel test rig (see Section 4).

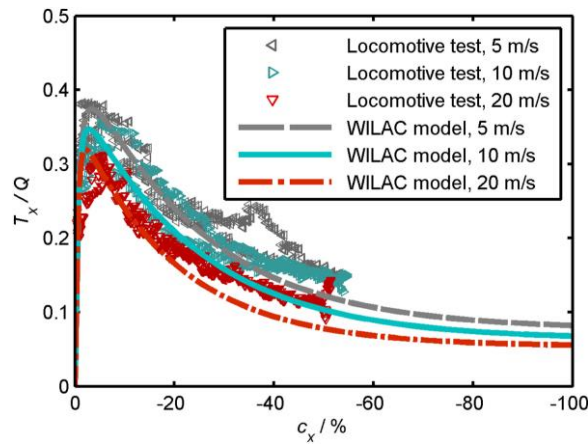


Fig. 9. Comparison of adhesion T_x/Q as a function of longitudinal creep c_x for different rolling speeds in dry surface condition: WILAC model results (lines), locomotive test data from literature [15] (marker).

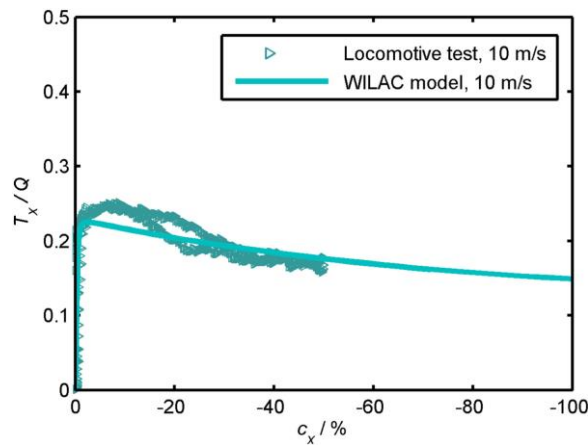


Fig. 10. Comparison of adhesion T_x/Q as a function of longitudinal creep c_x at 10 m/s rolling speed in wet surface condition: WILAC model result (line), locomotive test data from literature [15] (marker).

Fig. 11 demonstrates the change of adhesion as a function of rolling speed according to the original Polach model in comparison with the adhesion data from locomotive tests in dry surface condition. For this purpose the Polach parameters in the WILAC model for the adhesion curve at 10 m/s in Fig. 9 have been taken. These (fixed) Polach parameters have then been used to calculate the adhesion curves at 5 m/s and 20 m/s (with the linear regression models deactivated). The variation of the adhesion curve in Fig. 11 reflects thus purely the behaviour of the Polach model. A comparison of the WILAC adhesion curves in Fig. 9 (Linear regression models + Polach model) with the adhesion curves in Fig. 11 (Polach model with fixed Polach parameters) show that the change in adhesion with rolling speed in the creep range from approximately -10% to approximately -50% is too large in the Polach model when compared to locomotive test data. The adjustment of the (internal) Polach parameters by linear regression models in the WILAC model gives a better agreement with locomotive test data, as shown in Fig. 9.

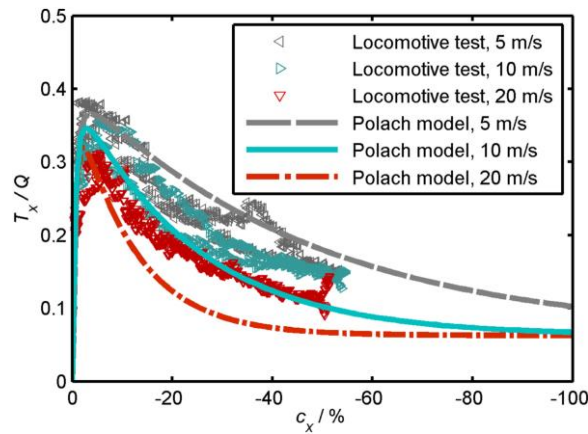


Fig. 11. Variation of adhesion T_x/Q calculated with the Polach model as a function of longitudinal creep c_x for different rolling speeds in dry surface condition (lines). The Polach parameters for the curve at 10 m/s have been used for calculating the Polach adhesion curves at 5 m/s and 20 m/s (with deactivated linear regression models). For comparison locomotive test data from literature [15] are also shown (marker).

6. Discussion

Experimental results from the tram wheel test rig show that the adhesion characteristic changes in a complex way with the water flow rate. The adhesion characteristic in damp condition is not just a linear interpolation between the adhesion curves observed in dry and in wet conditions.

The observed adhesion characteristic at a water flow rate of 25 $\mu\text{l/s}$ proves that low adhesion conditions can occur with only wear debris and little amounts of water present in the contact. Under the right set of conditions the adhesion drops to values of 0.06 at large creep without the presence of grease or oil. Increasing the water flow rate to 35 $\mu\text{l/s}$ changes the adhesion curve to the “wet” type with adhesion values of approximately 0.15 which can still be considered to be low adhesion. At a water flow rate of 60 $\mu\text{l/s}$ (see Fig. 3) the adhesion curve is already very similar to the adhesion curve at a water flow rate 350 $\mu\text{l/s}$. Thus a water flow rate of 60 $\mu\text{l/s}$ can be regarded as the upper limit of the range in which the water flow rate has a considerable influence on the adhesion characteristic.

At the tram wheel test rig only an accelerating wheel has been studied. However, a similar adhesion characteristic can be expected for a braking wheel if one assumes that the adhesion is independent of the direction of the relative motion between wheel and rail.

The above findings may be relevant for railway operation: If both rails are covered with wear debris over a certain distance and if the rail surface is just slightly wet (for example at the onset of rain, or in dew conditions) then the surface conditions may be comparable to the conditions at the tram wheel test rig at a water flow rate of 25 $\mu\text{l/s}$. If a constant braking torque is applied to the wheel in such a condition then the creep between wheel and rail will increase. If the working point exceeds the maximum adhesion value the creep will further increase and probably reach the low adhesion part of the adhesion curve. When the brakes are released the low adhesion condition may persist for some time because of the slow (re-)acceleration of the wheelset to rolling speed due to the small tangential friction forces in the contact.

The water flow rate is the only parameter related to the “wetness” of the surface in the WILAC model. When the model is used in engineering practice the water flow rate to the surface may be estimated from meteorological data such as the precipitation rate, humidity and temperature. Other parameters which certainly play a role in causing low adhesion conditions such as the surface roughness, or the amount and the composition of the interfacial layer on rails and wheels, are probably unknown in practice in most circumstances. Consequently, these are not input parameters for the WILAC model.

Hydrodynamic lubrication theory is not implemented directly in the WILAC model, which is based on boundary lubrication theory, although the WILAC model predicts adhesion in the presence of fluids. However hydrodynamic effects are indirectly considered in terms of the characteristics of the experimentally determined adhesion curves at the various water flow rates. This empirical approach adopted in the development of the WILAC model has the advantage that it results in a simple and computationally efficient engineering model in which the necessary input parameters are reduced to a minimum. Nevertheless the WILAC model is able to describe wheel/rail adhesion under a wide range of conditions ranging from dry to wet conditions including moist conditions.

The WILAC model may be implemented in multibody dynamics software to study the effect of low adhesion on train performance or it may be implemented in existing braking models to study braking strategies in moist conditions.

The modelling approach for predicting wheel/rail adhesion adopted for the WILAC model is not restricted to water and oxides in the contact. It can be extended to describe the influence of purposely added substances (such as friction modifier) on adhesion as well if the model development is accompanied by appropriate experiments.

7. Conclusions

Low amounts of water considerably influence the adhesion level and the shape of the adhesion curve. The adhesion curve in damp condition is not just a linear interpolation between the adhesion curve observed in dry condition and the adhesion curve observed in wet condition.

Adhesion values as low as 0.06 have been repeatedly observed in a tram wheel test rig experiment at high creep at a water rate of 25 $\mu\text{l/s}$ solely due to the presence of wear debris and water in the contact.

An engineering tool (WILAC model) has been developed which predicts the effect of water on wheel/rail adhesion in the whole range of conditions from dry over damp to wet. Main emphasis has been put on damp contact conditions.

WILAC model results agree with existing locomotive test data from literature in dry and wet conditions.

Acknowledgements

This work has been funded by the Rail Safety and Standards Board (RSSB) and Network Rail within the project T1077.

References

- [1] UIC 544-1. Bremse – Bremsleistung, International Union of Railways; 2004.
- [2] G. Vasic, F. Franklin, A. Kapoor, V. Lucanin. Laboratory simulation of low-adhesion leaf film on rail steel. *Int J Surf Sci Eng*, 2 (1/2) (2008), pp. 84–97
- [3] T1042. Investigation into the effect of moisture on rail adhesion, Rail Safety and Standards Board (RSSB); 2014.
- [4] P.M. Cann. The "leaves on the line" problem - a study of leaf residue film formation and lubricity under laboratory test conditions. *Tribol Lett*, 24 (2006), pp. 151–158
- [5] U. Olofsson, K. Sundvall. Influence of leaf, humidity and applied lubrication on friction in the wheel-rail contact: pin-on-disc experiments. *Proc Inst Mech Eng F: J Rail Rapid Transit*, 218 (2004), pp. 235–242

- [6] O. Arias-Cuevas, Z. Li, R. Lewis, E.A. Gallardo-Hernandez. Laboratory investigation of some sanding parameters to improve the adhesion in leaf contaminated wheel-rail contacts. *J Rail Rapid Transit Proc IMechE F*, 224 (2010), pp. 139–157
- [7] Z. Li, O. Arias-Cuevas, R. Lewis, E.A. Gallardo-Hernández. Rolling-sliding laboratory tests of friction modifiers in leaf contaminated wheel-rail contacts. *Tribol Lett*, 33 (2009), pp. 97–109
- [8] E.A. Gallardo-Hernandez, R. Lewis. Twin disc assessment of wheel/rail adhesion. *Wear*, 265 (2008), pp. 1309–1316
- [9] B.T. White, J. Fisk, M.D. Evans, A.D. Arnall, T. Armitage, D.I. Fletcher, R. Nilsson, U. Olofsson, R. Lewis. A study into the effect of the presence of moisture at the wheel/rail interface during dew and damp conditions. [submitted to] *J Rail Rapid Transit Proc IMechE F* (2016)
- [10] T.M. Beagley, C. Pritchard. Wheel/rail adhesion – the overriding influence of water. *Wear*, 35 (1975), pp. 299–313
- [11] G.W. Stachowiak, A.W. Batchelor. *Engineering Tribology*. Butterworth-Heinemann (2006)
- [12] Tomberger C, Rad-Schiene Der. *Kraftschluss unter Berücksichtigung von Temperatur, fluiden Zwischenschichten und mikroskopischer Oberflächenrauheit*, Technische Universität Graz; 2009.
- [13] O. Polach. Creep Forces in Simulations of Traction Vehicles Running on Adhesion Limit. *Wear*, 258, Elsevier (2005), pp. 992–1000
- [14] W. Zhang, J. Chen, X. Wu, X. Jin. Wheel/rail adhesion and analysis by using full scale roller rig. *Wear*, 253 (2002), pp. 82–88
- [15] K. Six, et al. Physical processes in wheel-rail contact and its implications on vehicle-track interaction. *Veh Syst Dyn: Int J Veh Mech Mobil*, 53 (2015), pp. 635–650
- [16] Y. Zhu, U. Olofsson, K. Persson. Investigation of factors influencing wheel–rail adhesion using a mini-traction machine. *Wear*, 292–293 (2012), pp. 218–231
- [17] H. Chen, M. Ishida, A. Namura, K.-S. Baek, T. Nakahara, B. Leban, M. Pau. Estimation of wheel/rail adhesion coefficient under wet condition with measured boundary friction coefficient and real contact area. *Wear*, 271 (2011), pp. 32–39
- [18] Kalker JJ, *On the Rolling Contact of Two Elastic Bodies in the Presence of Dry Friction*, Delft University of Technology; 1967.
- [19] E.A. Vollebregt. Numerical modeling of measured railway creep versus creep-force curves with CONTACT. *Wear*, 314 (2014), pp. 87–95
- [20] J.J. Kalker. A fast algorithm for the simplified theory of rolling contact. *Veh Syst Dyn*, 11 (1982), pp. 1–13
- [21] M. Spiryagin, O. Polach, C. Cole. Creep force modelling for rail traction vehicles based on the FASTSIM algorithm. *Veh Syst Dyn: Int J Veh Mech Mobil*, 51 (2013), pp. 1765–1783
- [22] Polach O, A fast wheel-rail forces calculation computer code. In: *Proceedings of the 16th IAVSD Symposium, Pretoria, August 1999, Vehicle System Dynamics Supplement*, 33, 728-739; 1999.
- [23] T.M. Beagley. The rheological properties of solid rail contaminants and their effect on wheel/rail adhesion
- [24] H. Chen, T. Ban, M. Ishida, T. Nakahara. Adhesion between rail/wheel under water lubricated contact. *Wear*, 253 (2002), pp. 75–81

- [25] H. Chen, M. Ishida, T. Nakahara. Analysis of adhesion under wet conditions for three-dimensional contact considering surface roughness. *Wear*, 258 (2005), pp. 1209–1216
- [26] Popovici R, *Friction in Wheel – Rail Contacts*, University of Twente, Enschede, The Netherlands; 2010.
- [27] A. Meierhofer. A New Wheel-Rail Creep Force Model based on Elasto-Plastic Third Body Layers [PhD Thesis] Graz University of Technology (2015)
- [28] Y. Zhu, U. Olofsson, A. Söderberg. Adhesion modeling in the wheel–rail contact under dry and lubricated conditions using measured 3D surfaces. *Tribol Int*, 61 (2013), pp. 1–10
- [29] P. Voltr, M. Lata. Transient wheel–rail adhesion characteristics under the cleaning effect of sliding. *Veh Syst Dyn*, 53 (2015), pp. 605–618